Structural Characterization of a Soluble Amyloid β-Peptide Oligomer

Liping Yu,[‡,§] Rohinton Edalji,[‡] John E. Harlan,[‡] Thomas F. Holzman,[‡,||] Ana Pereda Lopez,[‡] Boris Labkovsky,[#] Heinz Hillen,[⊥] Stefan Barghorn,[⊥] Ulrich Ebert,[⊥] Paul L. Richardson,[‡] Laura Miesbauer,[‡] Larry Solomon,[‡] Diane Bartley,[‡] Karl Walter,[‡] Robert W. Johnson,[‡] Philip J. Hajduk,[‡] and Edward T. Olejniczak*[,‡]

Pharmaceutical Discovery Division, GPRD, Abbott Laboratories, Abbott Park, Illinois 60064-6098, and Abbott GmbH and Co. KG, Ludwigshafen, Germany

Received November 3, 2008; Revised Manuscript Received January 2, 2009

ABSTRACT: Alzheimer's disease (AD) is a neurodegenerative disorder that is linked to the presence of amyloid β-peptides that can form insoluble fibrils or soluble oligomeric assemblies. Soluble forms are present in the brains and tissues of Alzheimer's patients, and their presence correlates with disease progression. Long-lived soluble forms can be generated in vitro by using small amounts of aliphatic hydrocarbon chains of detergents or fatty acids in preparations of amyloid β-peptides. Using NMR, we have characterized soluble oligomers of Aβ preglobulomer and globulomer that are stable and alter synaptic activity. The NMR data indicate that these soluble forms have a mixed parallel and antiparallel β-sheet structure that is different from fibrils which contain only parallel β-sheets. Using the structural data, we engineered a disulfide bond into the soluble Aβ globulomer to give a "new" soluble antigen that is stable, homogeneous, and binds with the same affinity to selective antibodies as the parent wt globulomer.

Alzheimer's disease (AD)[1] is a neurodegenerative disorder characterized by a progressive loss of cognitive abilities and by characteristic neuropathological features such as amyloid plaques, neurofibrillary tangles, and neuronal loss (*1*−*3*). The major component of brain amyloid plaques of AD is a 39 to 42 residue peptide termed amyloid β (Aβ) peptide, resulting from proteolytic processing of a larger amyloid precursor protein (APP). The insoluble amyloid fibril deposits of Aβ were thought to contribute to the progression of dementia of AD (*2*). However, a poor correlation was obtained between the insoluble deposits with the progression of AD (*4, 5*). In contrast, soluble Aβ oligomers have been found in the brain of AD patients (*6*), and the loss of synapses and cognitive perception seems to correlate better with soluble oligomers of Aβ(1−42) (*7, 8*). The cytotoxicity of Aβ has been postulated to relate to the soluble protofibrils that cause uncontrolled ion flux due to their pore-forming properties (*9, 10*). Moreover, soluble nonfibrillar oligomers of Aβ including amyloid-β-derived diffusible ligands (ADDL) (*11*) and globular β-amyloid species called globulomers (*12*) have been found to be highly toxic. Increasing evidence suggests that these early stage oligomers of Aβ may be important in AD.

Under most conditions, amyloid β-peptides rapidly convert into fibril forms. The fibril forms, which have been structurally characterized (*13*−*18*), have a cross-β structure that contains in-register parallel β-sheets (*14, 18*−*20*). Studies of amyloid intermediates indicate that they also have an ordered β-sheet structure (*21*). However, detailed structural characterization of these intermediates has been difficult because their levels are low and they are sensitive to solution conditions and only partially homogeneous. Recently, it was reported that the addition of detergent or fatty acid can result in long-lived soluble forms that are potent antigens in mice and rabbits for eliciting specific antibodies (*12*). These more stable soluble forms may be more amenable to detailed structural studies.

Here we have used solution NMR to study the soluble forms of Aβ called preglobulomers and globulomers that are more stable and alter synaptic activity (*12*). Our data are consistent with a model where the soluble form contains a mixed intermolecular parallel and intramolecular antiparallel β-sheet that is different from the all parallel amyloid β-peptides found in structural studies of fibrils (*15, 17, 18*). On the basis of these structural data, we engineered a disulfide bond into the soluble globulomer that locks the peptide into the intramolecular antiparallel β-sheet conformation. This "new" soluble amyloid β-peptide oligomer is still recognized by globulomer-selective antibodies with similar affinity as the parent. The structural features of this soluble form suggest that it can be targeted therapeutically independent of fibrillar forms.

* To whom correspondence should be addressed. Phone: (847) 223-7849. Fax: (847) 938-2478. E-mail: Edward.Olejniczak@abbott.com.
[‡] Abbott Laboratories.
[§] Current address: Carver College of Medicine, University of Iowa.
[||] Current address: Nanosphere Inc., Northbrook, IL.
[#] Abbott Bioresearch Center, Worcester, MA.
[⊥] Abbott GmbH and Co. KG.

[1] Abbreviations: AD, Alzheimer's disease; wt, wild type; APP, amyloid precursor protein; Aβ, amyloid β-peptide; MW, molecular weight; NMR, nuclear magnetic resonance; NOE, nuclear Overhauser effect; NOESY, nuclear Overhauser effect spectroscopy; TOCSY, total correlation spectroscopy; 2D, two dimensional; 3D, three dimensional; AFM, atomic force microscopy; HSQC, heteronuclear single-quantum coherence; SDS, sodium dodecyl sulfate; ADDL, amyloid-β-derived diffusible ligands; RMSD, root-mean-square deviation.

10.1021/bi802046n CCC: $40.75
Published on Web 02/13/2009

EXPERIMENTAL PROCEDURES

Cloning and Expression. Aβ peptide (1−42) was cloned and expressed in *Escherichia coli* BL21(DE3) cells using a pET29 vector. The cells were grown in flasks in M9 labeled media at 30 °C until the culture OD_{600nm} reached 0.45 and then expressed at 41 °C for 3 h by addition of 1 mM IPTG. The expressed peptide is located in the insoluble fraction after cell lysis. Purified amyloid β-peptide (MDAEFGHDSGFEVRHQKLVFFAEDVGSNKGAIIGLMVGGVVIA) exhibited an observed mass of 4645−4648 Da. This is consistent with the presence of N-terminal methionine as expected from the DNA expression sequence employed. Thus, compared with wt Aβ(1−42), this peptide expressed in *E. coli* contains an additional N-Met residue. The purified peptide was used to form globulomers (*12*). Details of preglobulomer and globulomer generation are given in the Supporting Information.

NMR. Labeled samples were prepared from cells grown in minimal media (*22*) using standard protocols (*23, 24*) and isotopes from Cambridge Isotope Laboratories. Uniformly ^{15}N-labeled samples were grown with 1 g/L $^{15}NH_4Cl$ and 3 g/L glucose in H_2O medium. Uniformly ^{15}N,^{2}H- and ^{14}N,^{2}H-labeled samples were grown with 3 g/L D-glucose-d_{12} in D_2O medium and by using 1 g/L $^{15}NH_4Cl$ and $^{14}NH_4Cl$, respectively. The uniformly ^{15}N,^{2}H,^{13}C-labeled sample was grown with 1 g/L $^{15}NH_4Cl$ and 3 g/L [^{13}C,^{2}H]glucose-d_{12} in 100% D_2O medium. The uniformly ^{15}N-labeled sample with selectively ^{13}C-labeled protonated methyl groups of Ile, Val, and Leu residues in a ^{2}H background was prepared by growing cells in media that contained 100% D_2O, D-glucose-d_{12} (3 g/L), and $^{15}NH_4Cl$ (1 g/L) and by supplementing media with [3-^{13}C]-α-ketobutyrate (50 mg/L for labeling isoleucine methyl groups) and [3,3-$^{13}C_2$]-α-ketoisovalerate (100 mg/L, for labeling valine and leucine methyl groups simultaneously). NMR preglobulomer samples contained 16 mg/mL peptide in ∼1.5% SDS-d_{25} and 1× phosphate-buffered saline at pH 7.4 (GIBCO).

NMR spectra were collected at 25 °C on Bruker DRX600 or DRX800 spectrometers. Resonances were assigned using a suite of backbone (*23*) and side chain ^{15}N- and ^{13}C-edited NOESY and TOCSY spectra (*25*). Backbone amide NH−NH NOEs were assigned from the 3D ^{15}N-resolved NOESY experiment by using a uniformly ^{15}N-labeled sample with selectively ^{13}C-labeled protonated methyl groups of Ile, Val, and Leu residues in a ^{2}H background. The ^{15}N-filtered and ^{15}N-edited 3D NOESY experiment was conducted as previously described (*26*) by using a mixed sample in which U-^{15}N,^{2}H-labeled and U-^{14}N,^{2}H-labeled samples were mixed at a 1:1 ratio. Distance constraints were obtained from the 3D ^{15}N- and ^{13}C-resolved NOESY experiment with mixing times from 80 to 200 ms.

Amide protection factors of N-Met-Aβ(1−42) globulomer samples were measured by comparing the amide peak intensities obtained for the sample in H_2O and the sample in D_2O after a period of amide exchange. Specifically, the N-Met-Aβ(1−42) globulomer samples were incubated in D_2O buffer at 4 °C, flash-frozen in liquid nitrogen to quench the H/D exchange, lyophilized, and redissolved in acidified DMSO-d_6. Control samples in H_2O buffer were subjected to the same protocol. Amide exchange rates of these samples were measured by collecting two-dimensional ^{15}N/^{1}H HSQC spectra within 3 min after dissolving the samples in acidified DMSO-d_6 (*13, 18*) where the peptide exists as a monomer and their NH cross-peaks can be easily assigned in the standard backbone experiments.

Structure Calculations. Models of a dimer repeating unit of the soluble N-Met-Aβ(1−42) preglobulomers were calculated using a simulated annealing protocol with the program CNX (*27, 28*). A total of 178 distance restraints derived from the analysis of the NMR data were included in the structure calculation. In addition, 44 φ angular restraints in the β-sheet regions were included in the structural calculations based on the analysis of C_α and C_β chemical shifts (*29*).

Atomic Force Microscopy (AFM). Tapping mode AFM images were collected on a Veeco/Digital Instruments nanoscope IIIa (Veeco, Santa Barbara, CA) at 4, 2, and 1 nm in both height and amplitude modes. Heights were determined using section analysis of the height mode image. Twenty microliters of globulomer at 0.029 mg/mL was deposited on $^1/_2$ in. diameter freshly cleaved Mica disks (Ruby Red Mica sheets; Electron Microscopy Sciences, Hatfield, PA) placed in a closed Petri dish with a damp paper towel, incubated for 7 min, and then rinsed with water and allowed to dry.

ELISA. The amyloid globulomers were diluted to 1.0 μg/mL in a coating buffer (100 mM $NaHCO_3$, pH 8.2). One hundred microliters of this solution was added to each well to be coated, and the wells were sealed with plate sealing film and left at 4 °C overnight. After the coating solution was removed, the wells were washed two to three times with 150 μL of PBST (Sigma PBS (P-3813) made with 0.05% Tween 20), and then 300 μL of blocking solution (3% nonfat dry milk (NFDM) in PBST) was added. The wells were then incubated for ∼2 h at room temperature with agitation. After the blocking solution was removed by washing the wells with 150 μL of PBST, 100 μL of primary antibody solutions with 0.04−100 μg/mL globulomer selective antibody (*12*) was added to the wells. The wells were then incubated for ∼2−3 h at room temperature with agitation. The primary antibody solutions were removed, and the wells washed 2–3 times with 150 μL of PBST. Then 200 μL of a 1:5000 dilution of donkey anti-mouse HRPO conjugate (Jackson Immuno Research) in 1% NFDM was added to each well. The wells were then incubated for ∼1 h at room temperature with agitation. Subsequently, the conjugate solution was removed, and wells washed 3 times with 200 μL of PBST. At this time 100 μL of HRPO substrate solution was added, and allowed to develop for at least 10 min. The reaction was stopped by the addition of 50 μL of 2 M H_2SO_4 and the absorbance of each well read at 450 nm using a microtiter-plate reader.

RESULTS AND DISCUSSION

Adding either fatty acid or hydrocarbon detergent to the preparations of N-Met-Aβ(1−42) peptides leads to the formation of stable and soluble aggregates whose oligomeric state depends on the amount of residual detergent (SDS) or lipid-like additive (*12*). In the presence of 0.2% SDS, the amyloid β-peptide forms a small soluble aggregate (referred to as N-Met-Aβ(1−42) preglobulomer) which can then be converted into a higher MW soluble aggregate (referred to

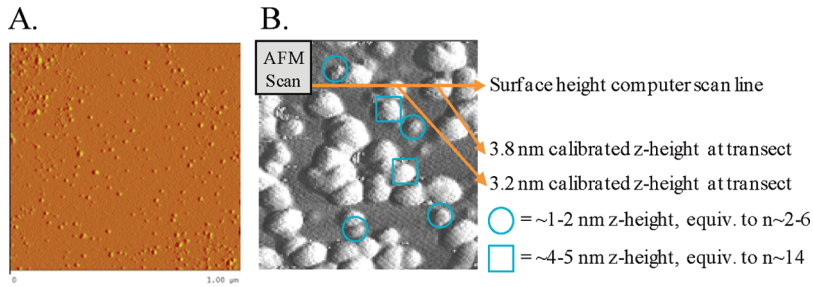

FIGURE 1: AFM images of the globulomer preparation of N-Met-Aβ(1−42) peptide. (A) Full AFM image and (B) expanded section. The globulomer preparation contains larger (4−5 nm high) species and smaller (1−2 nm high) species. The larger species are believed to be globulomers, while the smaller species are likely the preglobulomers observed by solution-state NMR in ~1.5% SDS. The sharpest features in the edge image data are lighter.

as N-Met-Aβ(1−42) globulomer) when the SDS concentration is diluted to 0.05% (*12*). Based on sedimentation studies (Supporting Information Figure 1), the N-Met-Aβ(1−42) preglobulomer has a MW of 16 kDa (corresponding to ~4 peptides/soluble aggregate), while the N-Met-Aβ(1−42) globulomer has a MW of ~64 kDa (corresponding to ~12−16 peptides/soluble aggregate). Small amounts of SDS, between 0.5 and 1.5 molecules of SDS per molecule of peptide, are bound or associated to the soluble globulomer based on radiolabeled detergent and size exclusion chromatography experiments (Supporting Information Figure 2). AFM images of the soluble N-Met-Aβ(1−42) globulomer preparation in Figure 1 show predominantly spherical oligomeric species with sizes ranging from 1−2 to 4−5 nm, consistent with the presence of both small N-Met-Aβ(1−42) preglobulomer and larger globulomer species. For the samples used in this study, we found that N-Met-Aβ(1−42) peptide behaves the same as synthesized wt Aβ(1−42) peptides. In particular, N-Met-Aβ(1−42) forms oligomers that are hydrodynamically the same, based on sedimentation velocity experiments, as the oligomers made from synthesized wt Aβ(1−42) peptides. N-Met-Aβ(1−42) peptides also form fibrils. Furthermore, samples made from the N-Met-Aβ(1−42) peptide are recognized by antibodies that also recognize wt Aβ(1−42). These antibodies include the commercially available 6E10 and our own globulomer-specific antibodies.

The soluble N-Met-Aβ(1−42) preglobulomer is amenable to direct structural studies by solution NMR. Figure 2 shows ^{15}N/^{1}HN HSQC spectra for the N-Met-Aβ(1−42) preglobulomer. The presence of a subset of strongly low-field-shifted amides (Figure 2A) and the observed slow hydrogen exchange of these amides (Figure 2B) indicate ordered structure for this portion of the preglobulomer sample. The C-terminal two residues may be important for the formation of this low-field-shifted and amide exchange protected species of preglobulomer since the shifted cross-peaks (Figure 2A) are not observed in the preparations using truncated N-Met-Aβ(1−40) (Figure 2C). The NMR spectra of soluble N-Met-Aβ(1−42) preglobulomer (Figure 2) has signals from both a well-structured segment and unstructured segment of the peptide based on their random coil chemical shifts. Our structural analysis is limited to peptide resonance connected to the well-dispersed amide signals.

The well-resolved amide peaks of the N-Met-Aβ(1−42) preglobulomer were assigned with a suite of backbone experiments (*23*) using uniformly ^{15}N,^{2}H,^{13}C-labeled N-Met-Aβ(1−42) peptide. The side chain resonances were assigned using ^{15}N- and ^{13}C-resolved 3D NOESY and TOCSY experiments. Selectively labeled samples were used to determine if NOE correlations were due to intramolecular or intermolecular NOEs. We used a ^{15}N-edited and ^{15}N-filtered NOE experiment (*26*) acquired on a sample of U-^{15}N,^{2}H-labeled and U-^{14}N,^{2}H-labeled N-Met-Aβ(1−42) peptides mixed at a 1:1 ratio before sample preparation to assign interpeptide chain NOE contacts between amides of a ^{15}N-labeled and unlabeled peptide. The NOEs for (G33 NH, L34 NH), (M35 NH, V36 NH), and (G37 NH, G38 NH) were observed in this experiment, indicating that these pairs of NH−NH NOEs are due to interchain contacts. In Figure 2D we show examples of these data obtained for (G37 NH, G38 NH). The strong (F19 NH, I32 NH) NOE was only observed in the regular ^{15}N-resolved 3D NOESY, indicating it is an intramolecular NOE. Additional interchain NH−CH_3 NOEs were assigned by using another mixed isotopic-labeled sample in which a U-^{15}N,^{2}H-labeled peptide was mixed at a 1:1 ratio with a U-^{14}N,^{2}H-labeled N-Met-Aβ(1−42) peptide selectively ^{13}C-labeled and protonated at methyl groups of IVL residues. The interchain NH−CH_3 NOEs between (G38 NH, V39 CH_3), (V39 NH, V39 CH_3), (M35 NH, V36 CH_3), and (L34 NH, L34 CH_3) were obtained from ^{15}N- and ^{13}C-resolved 3D NOESY experiments. In Figure 2E,F, we show the data obtained for (G38 NH, V39 CH_3) and (V39 NH, V39 CH_3). Additional intrachain NOEs were detected between (I32 NH, F19 $C_\beta H_2$), (I32 NH, F19 $C_\delta H_{1,2}$), (F19 NH, I32 $C_\beta H$), and (F19 NH, I32 $C_\gamma H_{1,2}$) and between residues A21 and A30.

The characteristic backbone atom chemical shifts, the protected amides, and the NOE data are all consistent with two β-strands from V18 to D23 and from K28 to V40 in the N-Met-Aβ(1−42) preglobulomer. Residues V18−D23 form one strand of an intrachain antiparallel β-sheet connected by a β-hairpin to the other intrachain strand K28−G33, while L34−V40 forms an interchain in-register parallel β-sheet. The NOE and amide protection data supporting this secondary structure are summarized in Figure 3A. One model that is consistent with our data is a peptide dimer repeating unit. A model for the peptide dimer was generated using the NOE-derived distance restraints, dihedral angle restraints based on backbone chemical shifts (*29*), and hydrogen bonds consistent with the amide protection data with the program CNX (*28*) using a simulated annealing protocol (*27*). A representative conformation of the peptide dimer is shown in Figure 3B. The ensemble of structures generated with these data resulted in a rmsd of 1.13 and 0.51 Å for the intrachain antiparallel β-sheet (19−32) and interchain in-register parallel

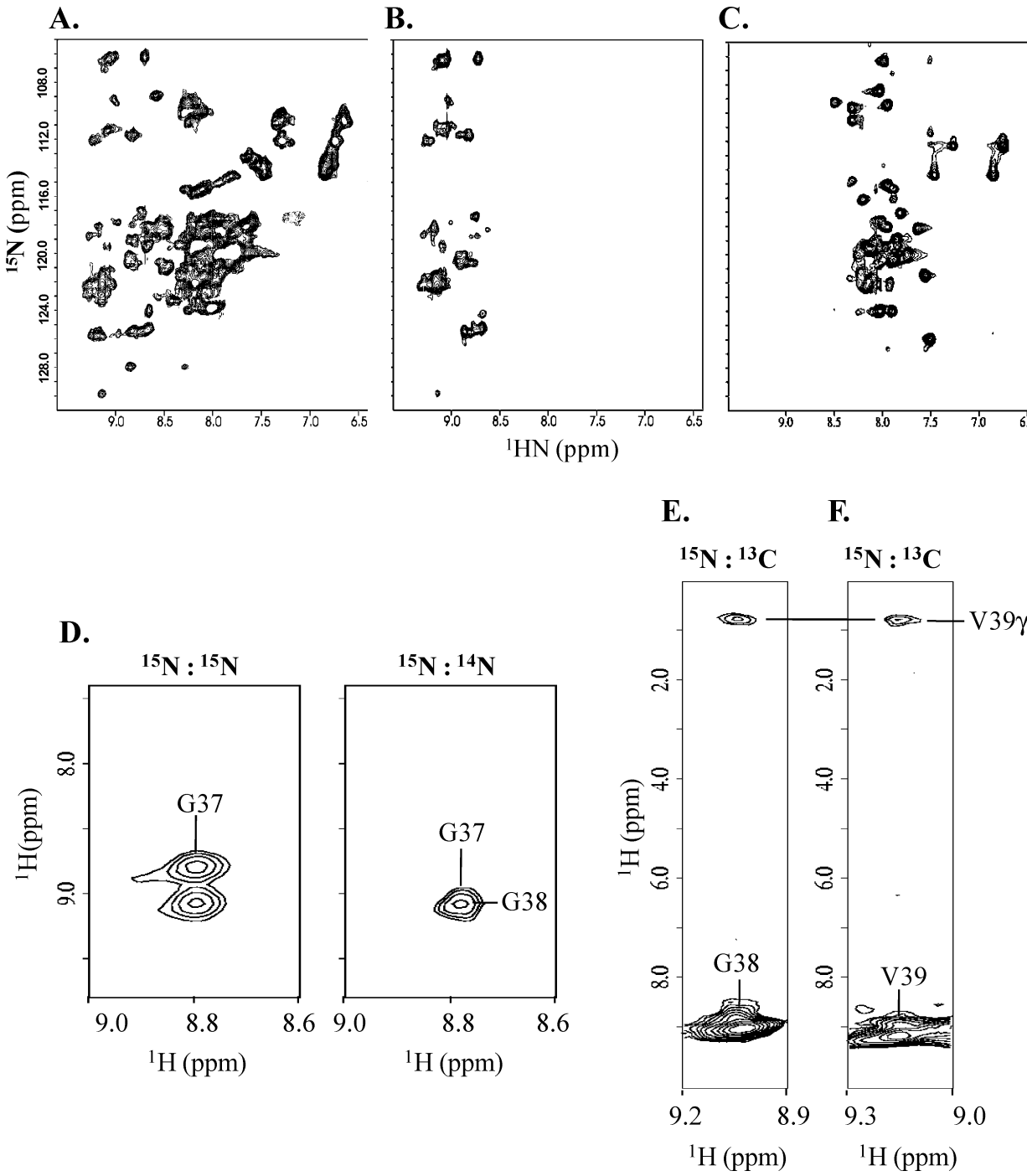

FIGURE 2: Panels A−C show ^{15}N/^{1}H HSQC spectra of the N-Met-Aβ peptide preglobulomer preparation. (A) N-Met-Aβ(1−42) peptide samples in 90% H_2O/10% D_2O buffer showing the well-dispersed amides between 8.5 and 9.5 ^{1}HN ppm. (B) The same sample after 18 h of amide exchange in 100% D_2O buffer. Only the well-dispersed amides observed in panel A remain. (C) Spectrum of N-Met-Aβ(1−40) peptides after preparation using the standard preglobulomer protocol. The low-field amides observed in panel A are completely absent in panel C. Panels D−F show NOE spectra of the N-Met-Aβ(1−42) preglobulomer samples. Interchain NOEs were assigned by using mixed isotopically labeled samples. (D) U-^{15}N,^{2}H-labeled and U-^{14}N,^{2}H-labeled peptides mixed at a 1:1 ratio. Left panel from ^{15}N-edited NOE experiment and right panel from ^{15}N-edited and filtered NOE experiment for (G37 NH, G38 NH). (E, F) U-^{15}N,^{2}H-labeled sample mixed at 1:1 ratio with U-^{14}N,^{2}H-labeled peptide selectively ^{13}C-labeled and protonated at methyl groups of IVL residues. (E) shows the interchain NH−CH_3 NOEs between G38 NH and V39 CH_3. (F) shows the interchain NH−CH_3 NOEs between V39 NH and V39 CH_3.

β-sheet (34−41), respectively. Our data do not constrain the relative orientation of the two β-sheet segments, leading to a backbone rmsd for the dimer ensemble (chains A, B residues 19−41) of 2.44 Å. A superposition of the 10 low-energy models consistent with the NMR data is given in Supporting Information Figure 3.

NMR spectra of the larger N-Met-Aβ(1−42) globulomer were not suitable for structural studies. However, we were able to measure protection factors for amide exchange by exchanging the globulomer sample into D_2O buffer, quenching the exchange, and then monitoring the peptide in DMSO under acidic conditions where the peptide is monomeric and able to be assigned using standard backbone experiments (*18, 30, 31*). Amide protection factors were measured from two-dimensional ^{15}N/^{1}H HSQC spectra collected within 3 min after dissolving in acidified DMSO-d_6 (pH 2.5). The amide protection data for

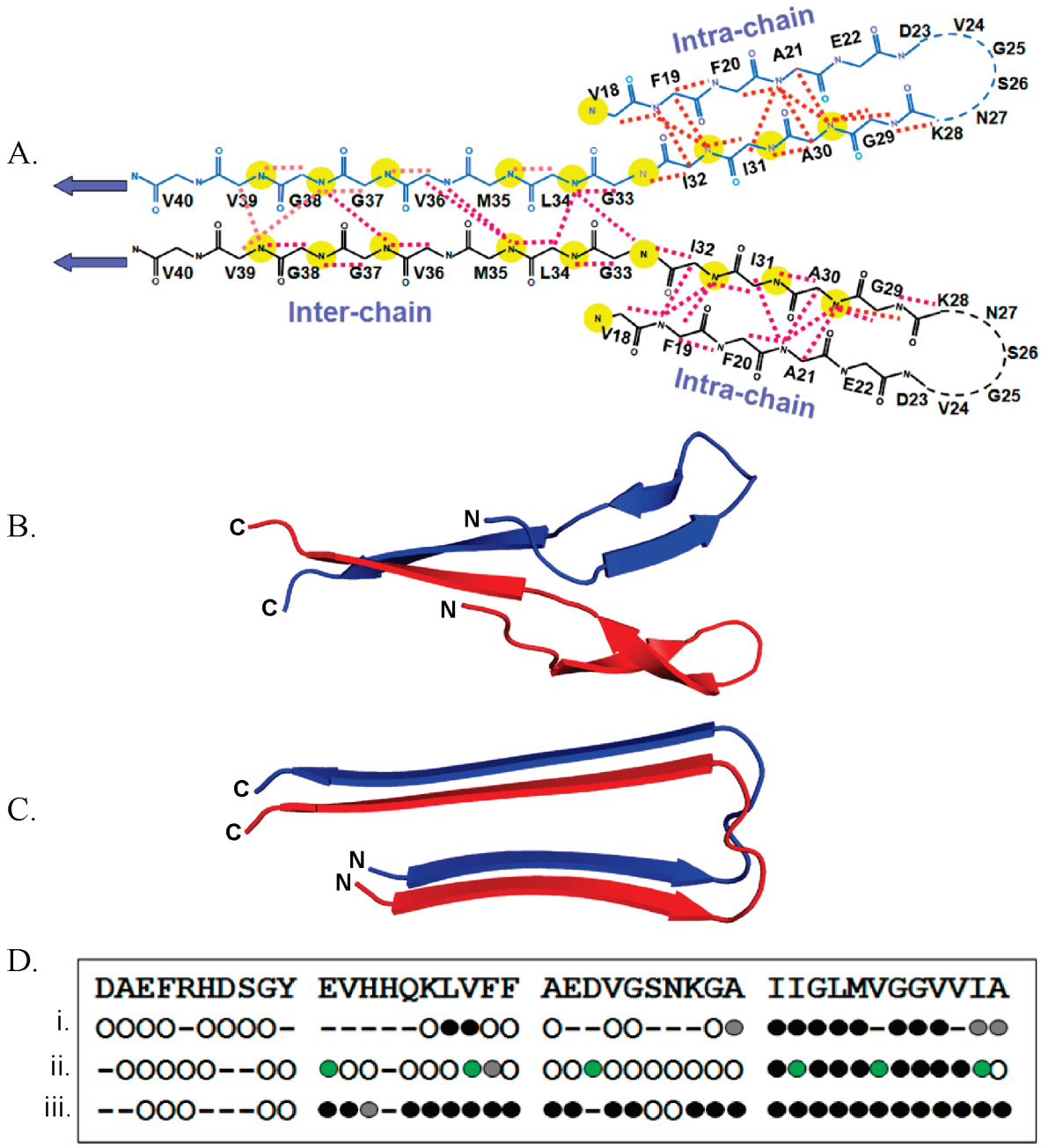

FIGURE 3: (A) Summary of NOE constraints obtained on the N-Met-Aβ(1−42) samples. Dashed lines indicate observed NOEs. Circles indicate the backbone amides that exhibit slow exchange in the NH/ND exchange experiments. (B) A representative low-energy structural model (residues 15−42) prepared with PyMOL (Delano Scientific LLC) that is consistent with the NMR data on the repeating unit of the β-amyloid peptide N-Met-Aβ(1−42) preglobulomer. The relative orientation of the two β-sheet segments is not well defined by the NMR data. (C) Two strands from the structure of Aβ(1−42) fibrils (residues 17−42) (PDB ID code 2BEG) (*18*) prepared with PyMOL (Delano Scientific LLC). (D) Comparison of backbone amide exchange protection for the (i) soluble N-Met-Aβ(1−42) preglobulomer, (ii) N-Met-Aβ(1−42) globulomer, and (iii) Aβ(1−42) fibrillar form (*13*). The backbone amides that exhibited slow, moderate, and fast exchange are indicated by black, gray, and white circles, respectively, below the sequence. The residues for which exchange rates could not be measured (including either not assigned or overlapped) are indicated by dashes. The sequence positions of the three pairs of overlapping cross-peaks of the amides in slow exchange in globulomer are indicated by green filled circles.

the N-Met-Aβ(1−42) preglobulomer and globulomer are shown in Figure 3D. For both preglobulomer and globulomer species, only the amides of residues 31−40 are fully protected, while rapid amide exchange is observed for all other measured amides except for 17−18 in the preglobulomer and a few residues whose cross-peaks are overlapped with the peaks for the residues from the C-terminal region of the globulomer. This exchange pattern is consistent with the hypothesis that both preglobulomer and globulomer adopt a similar secondary structure and that the N-Met-Aβ(1−42) globulomer is an oligomer of preglobulomer units. However, the amide exchange data (Figure 3D) of the N-Met-Aβ(1−42) preglobulomer and globulomer are very different from the fibril form (*13, 18*). In the fibril form, amides 11, 12, 15−22, 24, 25, and 28−30 are fully protected (*13*), while in the globulomer form, only the last 11 residues of the peptide are fully protected. The difference in the exchange rates between the fibril and N-Met-Aβ(1−42) globulomer form is consistent with the difference in the N-Met-Aβ(1−42) preglobulomer secondary structure and the structure reported for the fibril form.

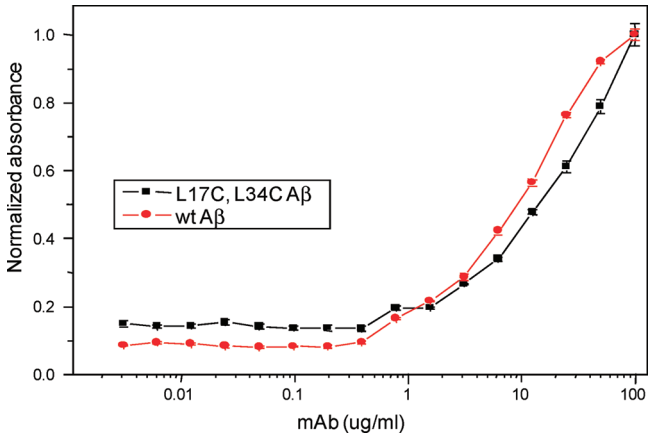

FIGURE 4: Comparison of direct ELISA assay of the wild-type and doubly mutated (L17C, L34C) N-Met-Aβ(1−42) peptide globulomers against an antiglobulomer-specific mAB (*12*).

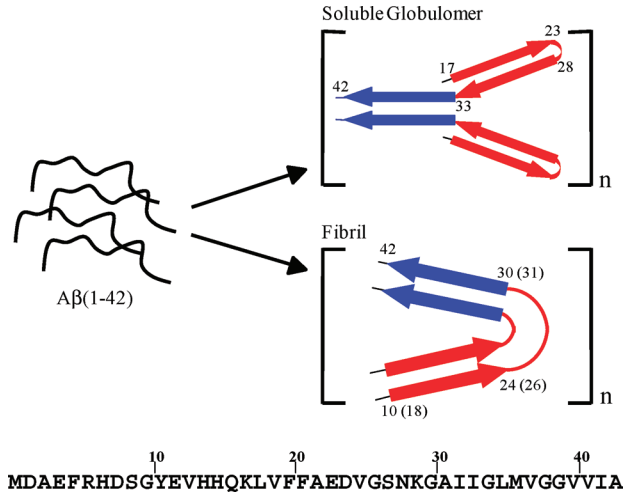

FIGURE 5: A schematic representation of the two stable forms of amyloid β-peptides (*12, 32, 37*). In both the soluble globulomer form and the insoluble fibril form, two-strand repeating units are shown, but the final forms are higher order oligomers (*n*-mers) of these units. The parallel β-sheet involving the hydrophobic C-terminus of the peptide and common to both forms is highlighted in blue. The segment distinct between the two forms is highlighted in red. The alternative starting and ending sequence numbers of the fibril form are indicated in parentheses.

To test the hypothesis that the quaternary structure of the N-Met-Aβ(1−42) globulomer consists of repeats of the preglobulomer dimer, we made a mutant peptide with an engineered disulfide bond that would lock the peptide into the antiparallel β-hairpin conformation that we have determined for the N-Met-Aβ(1−42) preglobulomer. Based on the structural model (Figure 3A,B), a L17C/ L34C double mutant amyloid β-peptide was made and used to form N-Met-Aβ(1−42) L17C/L34C globulomers. The globulomers of the mutant peptide were prepared by following the normal protocol except for the addition of 5 mM DTT at the beginning to prevent disulfide bond formation and a final step to remove DTT to allow a disulfide bond to form in the globulomer. The expected intrapeptide disulfide bond was confirmed based on mass spectrometric analysis where a nonreduced sample resulted in a 4622 Da mass which increased to 4624 Da upon reduction, consistent with a single intramolecular disulfide bond. The globulomers formed with the mutant peptides have a homogeneous size distribution in ultracentrifugation studies, similar to wild-type preparations. Furthermore, the mutant N-Met-Aβ(1−42) (L17C, L34C) globulomer binds with similar affinity as wild type to a globulomer-specific antibody (*12, 32*). As shown in Figure 4, the binding of this globulomer-specific antibody to the double mutant (L17C, L34C) and wild-type N-Met-Aβ(1−42) globulomer preparations are almost identical, indicating that the epitope is still properly displayed. Antibody recognition of this constrained Aβ globulomer analogue and the amide exchange data are both consistent with the hypothesis that globulomers are built from preglobulomer modules.

Aβ fibrils are composed of two in-register interstrand parallel β-sheets connected by a bend between residues 25 and 30 (*14, 18, 19*). In Figure 3B,C we compare the preglobulomer repeating unit to two strands of the fibril form of wt Aβ(1−42) (*14, 16, 18, 19*). Both structures exhibit an interstrand parallel β-sheet for the C-terminal residues (residues 34−42 in Aβ preglobulomers). However, in contrast to the fibril structure, the preglobulomers have an intrastrand antiparallel β-sheet connected by a β-hairpin between D23 and K28. Residues 10−16, which are part of the first β-sheet in fibrils (*14, 19*), are disordered in the preglobulomer.

It is likely that a bend versus a turn between residues 23 and 30 is the trait that leads to fibrils versus soluble globulomer. Residues in this region have been suggested to be critical for determining alternative conformations for the Aβ-peptide (*33*). Recent studies of truncated amyloid β-peptide (residues 21−30) found that in solution a β-hairpin structure is adopted (*34*). The stability of this β-structure was found to decrease in known familial amyloid β-peptide mutants, and it was hypothesized that the oligomerization propensity of the full peptide correlated with the turn stability of the model peptides (*35*).

The structural differences described here are consistent with a model for two distinct pathways for the amyloid Aβ soluble and insoluble peptides (*12, 32*). In this two-path model as depicted in Figure 5, the amyloid Aβ peptides derived from the cleavage of APP can form either soluble oligomers or fibrils. The initial peptides proceed to higher order oligomers to form fibrils or soluble globulomers based on the relative kinetic and thermodynamic stability of the bend (leading to fibrils) or the β-hairpin (leading to globulomers). Conditions that promote either structural feature (*36*), such as lipid composition (*12, 37*) or the effects of familial mutations (*38*), may result in changes in the ratio of soluble and insoluble forms of the peptide which may then influence disease.

CONCLUSIONS

We have used NMR to study specific soluble forms of amyloid β-peptide called preglobulomers and globulomers that are more stable and alter synaptic activity (*12*). Our structural characterization indicates that this class of soluble oligomers contains a peptide dimer-repeating unit, which is distinctly different from the fibril form. Using these data we demonstrated that a disulfide bond could be engineered into the soluble globulomer to give a "new" soluble antigen with similar affinity to selective antibodies as the parent. This

demonstrated that structural data can help to generate stable homogeneous soluble forms for further studies. Finally, the hydrogen exchange profile of this class of soluble oligomers can potentially be compared to that observed for different soluble oligomers. These data would complement using antibodies to structurally classify the various soluble oligomer forms (*39*).

SUPPORTING INFORMATION AVAILABLE

Additional details on Experimental Procedures; Figure 1, showing analytical ultracentrifugation sedimentation velocity and dynamic light-scattering (DLS) data of globulomers prepared from recombinant N-Met-Aβ(1−42); Figure 2, showing quantitation of binding of SDS to N-Met-Aβ(1−42) globulomers using ^{14}C-SDS; Figure 3, showing a superposition of 10 low-energy dimer repeating units of preglobulomer consistent with the NMR data. This material is available free of charge via the Internet at http://pubs.acs.org.

REFERENCES

1. Mattson, M. P. (2004) Pathways towards and away from Alzheimer's disease. *Nature 430*, 631–639.
2. Hardy, J., and Selkoe, D. J. (2002) The amyloid hypothesis of Alzheimer's disease: progress and problems on the road to therapeutics. *Science 297*, 353–356.
3. Klein, W. L., Krafft, G. A., and Finch, C. E. (2001) Targeting small Abeta oligomers: the solution to an Alzheimer's disease conundrum? *Trends Neurosci. 24*, 219–224.
4. Dickson, D. W., Crystal, H. A., Bevona, C., Honer, W., Vincent, I., and Davies, P. (1995) Correlations of synaptic and pathological markers with cognition of the elderly. *Neurobiol. Aging 16*, 285–298.
5. Terry, R. D., Masliah, E., Salmon, D. P., Butters, N., DeTeresa, R., Hill, R., Hansen, L. A., and Katzman, R. (1991) Physical basis of cognitive alterations in alzheimer's disease: Synapse loss is the major correlate of cognitive impairment. *Ann. Neurol. 30*, 572–580.
6. Kuo, Y.-M., Emmerling, M. R., Vigo-Pelfrey, C., Kasunic, T. C., Kirkpatrick, J. B., Murdoch, G. H., Ball, M. J., and Roher, A. E. (1996) Water-soluble Abeta(N-40, N-42) oligomers in normal and Alzheimer disease brains. *J. Biol. Chem. 271*, 4077–4081.
7. Lue, L.-F., Kuo, Y.-M., Roher, A. E., Brachova, L., Shen, Y., Sue, L., Beach, T., Kurth, J. H., Rydel, R. E., and Rogers, J. (1999) Soluble amyloid {beta} peptide concentration as a predictor of synaptic change in Alzheimer's disease. *Am. J. Pathol. 155*, 853–862.
8. McLean, C. A., Cherny, R. A., Fraser, F. W., Fuller, S. J., Smith, M. J., Beyreuther, K., Bush, A. I., and Masters, C. L. (1999) Soluble pool of Abeta amyloid as a determinant of severity of neurodegeneration in Alzheimer's disease. *Ann. Neurol. 46*, 860–866.
9. Arispe, N., Rojas, E., and Pollard, H. (1993) Alzheimer disease amyloid {beta} protein forms calcium channels in bilayer membranes: blockade by tromethamine and aluminum. *Proc. Natl. Acad. Sci. U.S.A. 90*, 567–571.
10. Lashuel, H. A., Hartley, D., Petre, B. M., Walz, T., and Lansbury, P. T. (2002) Neurodegenerative disease: Amyloid pores from pathogenic mutations. *Nature 418*, 291.
11. Lambert, M. P., Barlow, A. K., Chromy, B. A., Edwards, C., Freed, R., Liosatos, M., Morgan, T. E., Rozovsky, I., Trommer, B., Viola, K. L., Wals, P., Zhang, C., Finch, C. E., Krafft, G. A., and Klein, W. L. (1998) Diffusible, nonfibrillar ligands derived from Abeta 1−42 are potent central nervous system neurotoxins. *Proc. Natl. Acad. Sci. U.S.A. 95*, 6448–6453.
12. (a) Barghorn, S., Nimmrich, V., Striebinger, A., Krantz, C., Keller, P., Janson, B., Bahr, M., Schmidt, M., Bitner, R. S., Harlan, J., Barlow, E., Ebert, U., and Hillen, H. (2005) Globular amyloid beta-peptide oligomer—a homogenous and stable neuropathological protein in Alzheimer's disease. *J. Neurochem. 95*, 834–847. (b) Barghorn, S., Striebinger, A., Giaisi, S., Gaalen, M., Bespalov, A., Labkobsky, B., Ebert, U., and Hillen, H. (2008) in International Conference on Alzheimer's Disease 2008, Chicago, IL.
13. Olofsson, A., Sauer-Eriksson, A. E., and Ohman, A. (2006) The solvent protection of Alzheimer amyloid-{beta}-(1−42) fibrils as determined by solution NMR spectroscopy. *J. Biol. Chem. 281*, 477–483.
14. Petkova, A. T., Yau, W.-M., and Tycko, R. (2006) Experimental constraints on quaternary structure in Alzheimer's amyloid fibrils. *Biochemistry 45*, 498–512.
15. Makin, O. S., and Serpell, L. C. (2005) Structures for amyloid fibrils. *FEBS J. 272*, 5950–5961.
16. Ferguson, N., Becker, J., Tidow, H., Tremmel, S., Sharpe, T. D., Krause, G., Flinders, J., Petrovich, M., Berriman, J., Oschkinat, H., and Fersht, A. R. (2006) General structural motifs of amyloid protofilaments. *Proc. Natl. Acad. Sci. U.S.A. 103*, 16248–16253.
17. Eisenberg, D., Nelson, R., Sawaya, M. R., Balbirnie, M., Sambashivan, S., Ivanova, M. I., Madsen, A. O., and Riekel, C. (2006) The structural biology of protein aggregation diseases: Fundamental questions and some answers. *Acc. Chem. Res. 39*, 568–575.
18. Luhrs, T., Ritter, C., Adrian, M., Riek-Loher, D., Bohrmann, B., Dobeli, H., Schubert, D., and Riek, R. (2005) 3D structure of Alzheimer's amyloid-beta(1−42) fibrils. *Proc. Natl. Acad. Sci. U.S.A. 102*, 17342–17347.
19. Petkova, A. T., Ishii, Y., Balbach, J. J., Antzutkin, O. N., Leapman, R. D., Delaglio, F., and Tycko, R. (2002) A structural model for Alzheimer's beta-amyloid fibrils based on experimental constraints from solid state NMR. *Proc. Natl. Acad. Sci. U.S.A. 99*, 16742–16747.
20. Kirschner, D. A., Abraham, C., and Selkoe, D. J. (1986) X-ray diffraction from intraneuronal paired helical filaments and extraneuronal amyloid fibers in Alzheimer disease indicates cross-beta conformation. *Proc. Natl. Acad. Sci. U.S.A. 83*, 503–507.
21. Chimon, S., Shaibat, M. A., Jones, C. R., Calero, D. C., Aizezi, B., and Ishii, Y. (2007) Evidence of fibril-like beta-sheet structures in a neurotoxic amyloid intermediate of Alzheimer's beta-amyloid. *Nat. Struct. Mol. Biol. 14*, 1157–1164.
22. Sambrook, J., Fritsch, E. F., and Maniatis, T. (1989) *Molecular cloning—a laboratory manual*, Cold Spring Harbor Laboratory Press, New York.
23. Yamazaki, T., Lee, W., Arrowsmith, C. H., Muhandiram, D. R., and Kay, L. E. (1994) A suite of triple-resonance NMR experiments for the backbone assignment of ^{15}N, ^{13}C, ^{2}H-labeled proteins with high sensitivity. *J. Am. Chem. Soc. 116*, 11655–11666.
24. Goto, N. K., Gardner, K. H., Mueller, G. A., Willis, R. C., and Kay, L. E. (1999) A robust and cost-effective method for the production of Val, Leu, Ile (d1) methyl-protonated ^{15}N-, ^{13}C-, ^{2}H-labeled proteins. *J. Biomol. NMR 13*, 369–374.
25. Clore, G. M., and Gronenborn, A. M. (1994) Multidimensional heteronuclear magnetic resonance of proteins. *Methods Enzymol. 239*, 349–363.
26. Ikura, M., and Bax, A. (1992) Isotope-filtered 2D NMR of a protein-peptide complex: study of a skeletal muscle myosin light chain kinase fragment bound to calmodulin. *J. Am. Chem. Soc. 114*, 2433–2440.
27. Nilges, M., Clore, G. M., and Gronenborn, A. M. (1988) Determination of three-dimensional structures of proteins from interproton distance data by hybrid distance geometry-dynamical simulated annealing calculations. *FEBS Lett. 229*, 317–324.
28. Brunger, A. T., Adams, P. D., Clore, G. M., DeLano, W. L., Gros, P., Grosse-Kunstleve, R. W., Jiang, J. S., Kuszewski, J., Nilges, M., Pannu, N. S., Read, R. J., Rice, L. M., Simonson, T., and Warren, G. L. (1998) Crystallography & NMR system: A new software suite for macromolecular structure determination. *Acta Crystallogr. D54* (Part 5), 905–921.
29. Cornilescu, G., Delaglio, F., and Bax, A. (1999) Protein backbone angle restraints from searching a database for chemical shift and sequence homology. *J. Biomol. NMR 13*, 289–302.
30. Alexandrescu, A. T. (2001) An NMR-based quenched hydrogen exchange investigation of model amyloid fibrils formed by cold shock protein A. *Pacific Symp. Biocomput. 6*, 67–78.
31. Nishimura, C., Dyson, H. J., and Wright, P. E. (2005) Enhanced picture of protein-folding intermediates using organic solvents in H/D exchange and quench-flow experiments. *Proc. Natl. Acad. Sci. U.S.A. 102*, 4765–4770.
32. Gellermann, G. P., Byrnes, H., Striebinger, A., Ullrich, K., Mueller, R., Hillen, H., and Barghorn, S. (2008) A beta-globulomers are formed independently of the fibril pathway. *Neurobiol. Dis. 30*, 212–220.

33. Ma, B., and Nussinov, R. (2006) Simulations as analytical tools to understand protein aggregation and predict amyloid conformation. *Curr. Opin. Chem. Biol. 10*, 445–452.
34. Lazo, N. D., Grant, M. A., Condron, M. C., Rigby, A. C., and Teplow, D. B. (2005) On the nucleation of amyloid beta-protein monomer folding. *Protein Sci. 14*, 1581–1596.
35. Grant, M. A., Lazo, N. D., Lomakin, A., Condron, M. M., Arai, H., Yamin, G., Rigby, A. C., and Teplow, D. B. (2007) Familial Alzheimer's disease mutations alter the stability of the amyloid beta-protein monomer folding nucleus. *Proc. Natl. Acad. Sci. U.S.A. 104*, 16522–16527.
36. Chiti, F., Webster, P., Taddei, N., Clark, A., Stefani, M., Ramponi, G., and Dobson, C. M. (1999) Designing conditions for in vitro formation of amyloid protofilaments and fibrils. *Proc. Natl. Acad. Sci. U.S.A. 96*, 3590–3594.
37. Martins, I. C., Kuperstein, I., Wilkinson, H., Maes, E., Vanbrabant, M., Jonckheere, W., Van Gelder, P., Hartmann, D., D'Hooge, R., De Strooper, B., Schymkowitz, J., and Rousseau, F. (2008) Lipids revert inert Abeta amyloid fibrils to neurotoxic protofibrils that affect learning in mice. *Embo J. 27*, 224–233.
38. Selkoe, D. J. (2003) Folding proteins in fatal ways. *Nature 426*, 900–904.
39. Glabe, C. G. (2008) Structural classification of toxic amyloid oligomers. *J. Biol. Chem. 283*, 29639–29643.

BI802046N